Effects of Oxidative Stress on the Conjunctiva in Cu, Zn-Superoxide Dismutase-1 (*Sod1*)–Knockout Mice

Takashi Kojima,[1] Murat Dogru,[1,2] Osama M. A. Ibrahim,[1] Tais Hitomi Wakamatsu,[3] Masataka Ito,[4] Ayako Igarashi,[2] Takaaki Inaba,[1] Takahiko Shimizu,[5] Takuji Shirasawa,[6] Jun Shimazaki,[2] and Kazuo Tsubota[1]

[1]Department of Ophthalmology, Keio University School of Medicine, Tokyo, Japan
[2]Department of Ophthalmology, Tokyo Dental College, Chiba, Japan
[3]Department of Ophthalmology, São Paulo University School of Medicine, São Paulo, Brazil
[4]Department of Developmental Anatomy and Regenerative Biology, National Defense Medical College, Saitama, Japan
[5]Department of Advanced Aging Medicine, Chiba University Graduate School of Medicine, Chiba, Japan
[6]Department of Aging Control Medicine, Juntendo University Graduate School of Medicine, Tokyo, Japan

Correspondence: Murat Dogru, Ocular Surface and Visual Optics Department, Keio University School of Medicine, Shinanomachi 35, Shinjuku-ku, Tokyo 160-8582, Japan; muratodooru2012@yahoo.com.

Submitted: September 29, 2015
Accepted: November 5, 2015

Citation: Kojima T, Dogru M, Ibrahim OMA, et al. Effects of oxidative stress on the conjunctiva in Cu, Zn-superoxide dismutase-1 (*Sod1*)–knockout mice. *Invest Ophthalmol Vis Sci*. 2015;56:8382–8391. DOI:10.1167/iovs.15-18295

Purpose. A healthy conjunctiva secreting mucins is essential for maintaining the integrity of the ocular surface epithelium. We used Cu, Zn-superoxide dismutase 1–deficient mice (*Sod1*$^{-/-}$ mice) and investigated the effect of oxidative stress on the tear function, conjunctival phenotype, and ocular surface mucin expression.

Methods. Fifty-week-old C57/B6 wild-type (WT) and *Sod1*$^{-/-}$ mice were used for evaluations of the tear film breakup time and periodic acid Schiff staining of the conjunctival specimens to detect goblet cell densities in the conjunctiva. Immunohistochemistry stainings with anti-Muc5AC, anti-Muc1, anti–4-hydroxy-2-nonenal, and anti–8-hydroxy-2′-deoxyguanosine antibodies were also performed. The mRNA expression levels of Muc1, Muc5AC, Spdef, involcurin, and transglutaminase 1 were quantified with real-time RT-PCR.

Results. The mean goblet cell density in the aged *Sod1*$^{-/-}$ mice was significantly lower than the aged WT mice. The mean number of Muc5ac-positive cells was significantly lower in the aged *Sod1*$^{-/-}$ mice compared with the aged WT mice. The conjunctival epithelium in the aged *Sod1*$^{-/-}$ mice displayed marked staining with lipid and DNA oxidative stress markers. The mRNA expression of transglutaminase 1 and involcurin in the aged *Sod1*$^{-/-}$ mice was significantly higher than the aged WT mice. The Spdef mRNA expression in the aged *Sod1*$^{-/-}$ mice was also significantly lower than the aged WT mice.

Conclusions. Elevated oxidative stress status appears to affect the conjunctival differentiation and alter the conjunctival epithelial phenotype with aging in the *Sod1*$^{-/-}$ mice.

Keywords: oxidative stress, conjunctiva, mucin, *Sod1*

The conjunctival epithelium is composed of stratified nonkeratinizing cells that cover the ocular surface. Conjunctiva is essential to attain a healthy ocular surface and to maintain the visual function. In the forniceal conjunctiva, goblet cells are densely located and secret mucin including Muc5ac, which stabilizes the tear film. Conjunctival epithelium also expresses membrane-tethered mucins, which alter the conjunctival surface wettability.

The prevalence of dry eye disease varies between 7.8% and 14.6% based on the large epidemiologic studies in the United States.[1] Dry eye, which could deteriorate visual function,[2] has been reported to be a major public health issue and have an important impact on quality of life.[3,4]

In the 2007 International Dry Eye Workshop (DEWS) report, the core mechanisms of dry eye are explained by tear hyperosmolarity and tear film instability.[5] Tear film instability can lead to irregular astigmatism and increased higher-order aberrations, resulting in decreased visual functions.[2,6]

Aging has been reported to result from deleterious damage to cells and tissues by free radicals. An imbalance between cell damage by free radicals and radical-scavenging antioxidant systems results in a condition that is called oxidative stress, which is associated with many age-related diseases and is also considered as a major factor in the process of senescence.[7] Superoxide dismutase (SOD) is one of the well-known antioxidant systems, and SOD is composed of three isozymes: SOD1, SOD2, and SOD3. Among them, SOD1 is widely distributed in the tissues and represents 90% of the total SOD activity.[8,9] We previously showed that Cu, Zn-Sod knockout (*Sod1*$^{-/-}$) mice had decreased tear secretion with lacrimal gland and ocular surface damage and concluded that *Sod1*$^{-/-}$ mice are a good model for studying age-related dry eye disease.[10]

Conjunctival alterations in the *Sod1*$^{-/-}$ mice have not been studied in detail thus far. It has been reported that the differentiation into goblet cells in the mouse tracheobronchial and gastrointestinal epithelium is highly regulated by sterile alpha motif (SAM)-pointed domain epithelial-specific transcription factor (Spdef). A recent study showed that Spdef is also required for conjunctival goblet cell differentiation and that *Spdef*$^{-/-}$ mice have significantly increased corneal surface fluorescein staining.[11]

In the current study, we investigated the age-related tear film and conjunctival changes including conjunctival differentiation and transmission electron microscopy in *Sod1*$^{-/-}$ mice.

Methods

Ethics Statement

All studies were performed in accordance with the ARVO Statement for the Use of Animals in Ophthalmic and Vision Research. The study was approved by Tokyo Dental College Ichikawa Hospital Ethics Committee for Animal Research.

Animals

Seventeen *Sod1*$^{-/-}$ male mice with a C57BL6 background and 14 C57BL6 strain wild-type (WT) male mice were examined at 10 and 50 weeks in this study. The *Sod1*$^{-/-}$ mice were from the Tokyo Metropolitan Institute of Gerontology and the WT C57BL/6 mice were purchased from Japan Clea (Osaka, Japan).

Measurement of Tear Film Breakup Time

After instillation of 1 μL 0.5% sodium fluorescein, excess fluorescein was wiped away. After spontaneous blinking, the time until the appearance of a dark area representing tear film breakup (BUT) was measured three times, and the averaged value was used for analysis.

Conjunctival Specimen Collections

Animals were euthanized using a combination of 6 mg/mL ketamine and 4 mg/mL xylazine at 10 and 50 weeks. The conjunctiva was removed from the eyeball using a fine scissors and forceps. Samples were divided and fixed in 4% buffered paraformaldehyde for stainings, stored in 2.5% glutaraldehyde in 0.1 M phosphate for electron microscopy, RNAlater (Applied Biosystems, Carlsbad, CA, USA) for RT-PCR, or Tissue-Tek Optimal Cutting Temperature (OCT) compound (Sakura Finetek, Tokyo, Japan) for immunohistochemistry.

Histolopathologic Assessment of Conjunctival Specimens

All conjunctival specimens for immunohistochemistry detecting ocular surface mucins were immediately stored in OCT. The frozen OCT blocks were cut at a thickness of 6 μm. To evaluate the goblet cells, conventional periodic acid Schiff (PAS) staining was performed.

Goblet Cell Density Quantifications

Five randomly selected nonoverlapping areas in each specimen from the inferior eyelid in 890 × 705-μm frames were digitally photographed (Axioplan2 imaging; Carl Zeiss, Jena, Germany). A total of five images from each *Sod1*$^{-/-}$ or WT mice were taken where the photographer was masked to the mouse genetic information. The number of goblet cells per section was counted manually, and scores from the samples were determined for mean goblet cell density calculations.

Fluorescent Immunohistochemistry Staining for the Ocular Surface Mucins

To evaluate the localization and expression levels of Muc1and Muc5ac in the ocular surface, fluorescent immunohistochemistry was performed as follows: briefly, cryosections (6 μm) from the mouse eyeball were fixed in 4% paraformaldehyde for 20 minutes. After blocking with 1% BSA PBS containing 2% donkey serum, sections were incubated overnight with primary antibodies. After washing with PBS, the sections were incubated for 30 minutes with secondary antibodies and observed using a fluorescence microscope (Carl Zeiss). For negative controls, isotype control IgG was applied instead of primary antibody. The specimens were immunostained with the following primary antibodies: mouse anti-Muc5ac antibody (2 μg/mL, 14-0041, MS-145-P0; Thermo, Cheshire, UK) and rabbit anti-Muc1 (0.2 mg/mL, ab8878; Abcam, Cambridge, MA, USA). The secondary antibody was fluorescein isothiocyanate–conjugated anti-rabbit IgG antibody (0.0075 mg/mL; Jackson Immunoresearch Laboratories, West Grove, PA, USA). DAPI (4′-6-diamidino-2-phenylindole; Vector Laboratories, Burlingame, CA, USA) was used for nuclear staining.

Immunohistochemistry Staining for Oxidative Stress Markers

Oxidative stress–induced lipid peroxidation was assessed by immunohistochemical detection of 4-hydroxy-2-nonenal (4-HNE); 4-HNE is a well-known major lipid peroxidation product. Oxidative DNA damage was investigated by immunohistochemical staining with anti–8-hydroxy-2′-deoxyguanosine (8-OHdG) antibodies. The avidin–biotin–peroxidase complex method was used in immunostainings. Tissues were fixed overnight in a 4% buffered paraformaldehyde solution and processed for paraffin embedding. Four-micrometer sections were cut from paraffin wax blocks, mounted on precoated glass slides, deparaffinized, and rehydrated. To block nonspecific background staining, conjunctival sections were treated with normal horse serum (Vector Laboratories) for 2 hours at room temperature. An antigen unmasking procedure was not performed. The tissues were then treated with mouse anti–8-OHdG monoclonal antibodies at a concentration of 10 μg/mL diluted with horse blocking serum (Japan Institute for the Control of Aging [JaICA], Shizuoka, Japan) and anti–4-HNE monoclonal antibodies at a concentration of 25 μg/mL diluted with horse blocking serum (JaICA) for 2 hours at room temperature. For the negative controls, the primary antibody was replaced with mouse IgG1 Isotype control (MOPC-21; Sigma-Aldrich Corp., St. Louis, MO, USA). Endogenous peroxidase activity was blocked using 3.0% H_2O_2 in methanol for 3 minutes. The sections were incubated for 30 minutes with biotin-labeled horse anti-mouse IgG serum (Vector Laboratories), followed by avidin–biotin–alkaline phosphatase complex treatment (Vector Laboratories) for 30 minutes. The sections were washed in PBS buffer, developed in prepared 3,3′-diaminobenzidine chromogen solution (Vector Laboratories), lightly counterstained with hematoxylin for 4 minutes at room temperature, washed with tap water, dehydrated, and mounted.

Transmission Electron Microscopic Examination

Conjunctival specimens were immediately fixed with 2.5% glutaraldehyde in 0.1 M PBS (pH 7.4), immersed for 4 hours at 4°C, and washed three times with a 0.1 M PBS solution. The samples were then postfixed in 2% osmium tetroxide, dehydrated in a series of ethanol and propylene oxide, and embedded in epoxy resin. One-micrometer sections were stained with methylene blue, and the conjunctival tissues were thin sectioned on an ultratome (LKB, Gaithersburg, MD, USA) with a diamond knife. Sections were collected on 150-mesh grids, stained with uranyl acetate and lead citrate, examined, and photographed using an electron microscope (model 1200 EXII; JEOL, Tokyo, Japan).

Investigative Ophthalmology & Visual Science

Quantitative RT-PCR for Ocular Surface Mucin and Spdef

Mouse conjunctival tissues were preserved overnight in RNA later (Applied Biosystems) after prompt excision. Tissues were then transferred into ISOGEN (Nippon Gene, Tokyo, Japan) and homogenized well. Total RNA was extracted, cleaned up, and treated with DNase using the RNeasy mini kit (Qiagen, Valencia, CA, USA). cDNA synthesis was performed using the iScript cDNA Synthesis Kit (Bio-Rad, Hercules, CA, USA). SYBR Green–based quantitative real-time PCR was performed using StepOnePlus system (Applied Biosystems). Mouse glyceraldehyde-3-phosphate (GAPDH) (sense 5′-TGA CGT GCC GCC TGG AGA AA-3′, antisense, 3′-AGT GTA GCC CAA GAT GCC CTT CAG-5′), Muc1(sense 5′-CTT TCA GAA GAC TCC GCC AG-3′, antisense 3′-GGC CAA GAC TGA TTC AGA GC-5′), Muc5ac (sense 5′-AAA GAC ACC AGT AGT CAC TCA GCA A-3′, antisense 3′-CTG GGA AGT CAG TGT CAA ACC A-5′), transglutaminase 1 (sense 5′-AAA GAC ACC AGT AGT CAC TCA GCA A-3′, antisense 3′-AAC TCA TCC GTG TGG TGC TC-5′), and Spdef (sense 5′-TTG GAT GAG CAC TCG CTA GA-3′, antisense 3′-AAA AGC CAC TTC TGC ACG TT-5′) primers were used. Data were normalized to GAPDH.

Statistical Analyses

The Mann-Whitney *U* test was performed to compare the tear film break-up time (TBUT), staining area, goblet cell density, and mRNA expression level between different mice groups. $P < 0.05$ was considered statistically significant. SPSS ver.19 (IBM Corp., New York, NY, USA) software was used for all statistical analyses.

Results

Lack of SOD1 Accelerates Ocular Surface Damage and Deteriorates Tear Functions

To evaluate tear functions, the cotton thread test and BUT measurements were performed. Although there was no significant difference in weight-adjusted tear volume between the 10-week-old WT and 10-week-old *Sod1*$^{-/-}$ mice, the tear volume in the 50-week-old *Sod1*$^{-/-}$ mice was significantly lower than the 50-week-old WT mice (Supplementary Table S1). The mean BUT values in the 10-week-old WT and *Sod1*$^{-/-}$ mice were 3.2 ± 1.6 and 3.0 ± 1.7 seconds, respectively. There was no significant difference in the BUT values between the 10-week-old WT and the 10-week-old *Sod1*$^{-/-}$ mice ($P = 0.7865$). The mean BUT values in the 50 week-old wild and *Sod1*$^{-/-}$ mice were 3.2 ± 1.2 and 2.1 ± 1.1 seconds, respectively. The mean BUT values in the 50-week-old *Sod1*$^{-/-}$ mice were significantly shorter than the 50-week-old WT mice ($P = 0.0149$) (Fig. 1A). Fluorescein staining was performed to evaluate the ocular surface damage. There was no significant difference in the mean fluorescein staining scores between the 10-week-old WT and 10-week-old *Sod1*$^{-/-}$ mice ($P = 0.3552$). The mean fluorescein staining scores in the 50-week-old *Sod1*$^{-/-}$ mice was significantly higher than the 50-week-old WT mice ($P = 0.0015$; Supplementary Table S1).

Lipid and DNA Oxidative Damage Accumulated With Aging in the Mouse Conjunctival Tissue

To evaluate the influence of oxidative stress on nuclei, we performed immunohistochemistry stainings with a DNA oxidative stress marker: anti–8-OHdG (Fig. 1B). Specimens from the 50-week-old *Sod1*$^{-/-}$ mice exclusively showed dense staining in the nuclei of the conjunctival epithelium compared with the specimens from the WT mice at 10 and 50 weeks and *Sod1*$^{-/-}$ mice at 10 weeks (Fig. 1B). The mean (μm^2) of the positively stained areas with 8-OHdG antibodies was 3044 ± 1578 for WT mice at 10 weeks, 9754 ± 2403 for *Sod1*$^{-/-}$ mice at 10 weeks, 9047 ± 2795 for WT mice at 50 weeks, and 38,766 ± 4578 for *Sod1*$^{-/-}$ mice at 50 weeks. The extent of conjunctival staining with 8-OHdG antibodies showed a significant increase ($P < 0.0001$) in both *Sod1*$^{-/-}$ and WT mice from 10 to 50 weeks as shown in Figure 1C. Moreover, the extent of staining with 8-OHdG antibodies in the *Sod1*$^{-/-}$ mice at 50 weeks was significantly higher ($P < 0.0001$) than the WT mice at 50 weeks (Fig. 1C). To evaluate the lipid oxidative stress in conjunctival tissues, we performed immunohistochemistry stainings with an anti–4-HNE antibody. Specimens from the 50-week-old *Sod1*$^{-/-}$ mice extensively showed dense staining in the conjunctival epithelium compared with the specimens from the WT mice at 10 and 50 weeks and *Sod1*$^{-/-}$ mice at 10 weeks (Fig. 1D). The mean (μm^2) of the positively stained areas with 4-HNE antibodies in the conjunctival epithelium was 4676 ± 1678 for WT mice at 10 weeks, 15,478 ± 2506 for *Sod1*$^{-/-}$ mice at 10 weeks, 24,689 ± 2899 for WT mice at 50 weeks, and 60,453 ± 8823 for *Sod1*$^{-/-}$ mice at 50 weeks. The extent of conjunctival staining with 4-HNE antibodies showed a significant increase ($P < 0.0001$) in both *Sod1*$^{-/-}$ and WT mice from 10 to 50 weeks as shown in Figure 1E. Moreover, the extent of staining with 4-HNE antibodies in the *Sod1*$^{-/-}$ mice at 50 weeks was significantly higher ($P < 0.0001$) than the WT mice at 50 weeks (Fig. 1E).

Aging Was Associated With a Decrease of Goblet Cells in the Conjunctival Epithelium in *Sod1*$^{-/-}$ Mice

Conjunctival goblet cells were evaluated with PAS staining. In the 50-week-old *Sod1*$^{-/-}$ mice, a marked decrease of goblet cells and thickening of conjunctival epithelium were observed (Fig. 2A). The mean number of goblet cells was 56.3 ± 28.5 for WT mice at 10 weeks, 48.8 ± 24.2 for *Sod1*$^{-/-}$ mice at 10 weeks, 48.3 ± 13.6 for WT mice at 50 weeks, and 16.9 ± 10.2 for *Sod1*$^{-/-}$ mice at 50 weeks. The mean goblet cell density in the conjunctiva showed a significant decrease ($P < 0.0001$) in the *Sod1*$^{-/-}$ mice from 10 to 50 weeks as shown in Figure 2B ($P = 0.0002$). Moreover, the goblet cell density in the *Sod1*$^{-/-}$ mice at 50 weeks was significantly lower ($P < 0.0001$) than the WT mice at 50 weeks (Fig. 2B).

Aged *Sod1*$^{-/-}$ Mice Showed Alterations in the Ocular Surface Mucin Expression

To evaluate the membrane tethered mucins, Muc1 immunohistochemistry using an anti-Muc1 antibody was performed. The conjunctival tissue in the 10-week-old WT and *Sod1*$^{-/-}$ mice showed a continuous positive staining pattern in the superficial conjunctival epithelium. Fifty-week-old WT mice also showed a similar immunohistochemical expression. On the other hand, 50-week-old *Sod1*$^{-/-}$ mice showed marked less staining in the conjunctival epithelium (Fig. 3A). Real-time RT-PCR of the conjunctival tissues showed that Muc1 mRNA expression in the 50-week-old *Sod1*$^{-/-}$ mice was significantly lower than the 50-week-old WT mice (Fig. 3B; $P = 0.0003$).

To evaluate the secretory mucin, Muc5ac, immunohistochemistry using an anti-Muc5ac antibody was performed. The conjunctival tissues in the 10- and 50-week-old WT and 10-

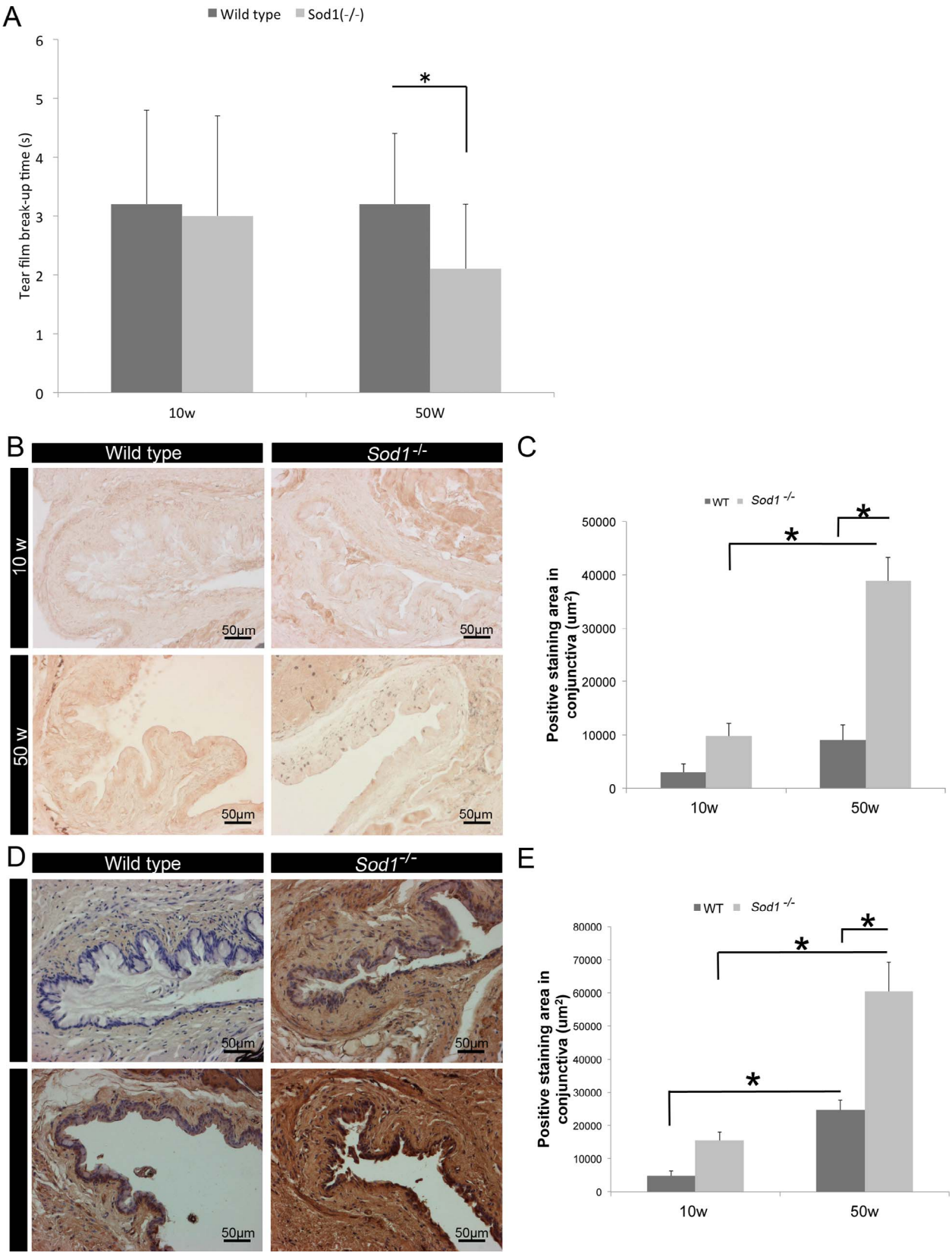

Figure 1. Tear film stability, oxidative DNA, and lipid changes in the conjunctival tissues. (**A**) Tear film BUT was measured to evaluate the tear film stability. The mean tear film BUT in 50-week-old *Sod1*$^{-/-}$ mice was significantly shorter than the 50-week-old WT mice. (**B**) Conjunctival epithelial cell nuclei showed scanty staining with 8-OHdG antibodies in the *Sod1*$^{-/-}$ and WT mice at 10 weeks. There was a marked increase in nuclear staining from 10 to 50 weeks, exclusively in all *Sod1*$^{-/-}$ mice. Relatively more conjunctival epithelial cell nuclei stained with anti–8-OHdG antibodies in the *Sod1*$^{-/-}$ mice at 50 weeks compared with conjunctival specimens from WT mice at 50 weeks. (**C**) Semiquantitative analysis of the extent of conjunctival epithelial cell staining for 8-OHdG showed a statistically significance increase in the 50-week-old mice group compared with

Investigative Ophthalmology & Visual Science

the 10-week-old group and a significant elevation in staining for the *Sod1*$^{-/-}$ group compared with the WT mice at 50 weeks. *Error bars* indicate SD from at least five independent samples. (**D**) Late-phase lipid peroxidation marker 4-HNE stained conjunctival epithelial cells positively showing a dense staining in the 50-week-old *Sod1*$^{-/-}$ mice. The WT mice in the 50-week-old specimens were also stained but not to the extent observed in *Sod1*$^{-/-}$ mice. Hematoxylin staining was performed for counterstaining. (**E**) Semiquantitative analysis of the extent of conjunctival epithelial cell staining for 4-HNE showed a statistically significance increase in the 50-week mice group compared to the 10-week group and a significant elevation in staining for the *Sod1*$^{-/-}$ group compared with the WT mice at 50 weeks. *Error bars* indicate SD from at least five independent samples. *$P < 0.05$.

week-old *Sod1*$^{-/-}$ mice showed abundant positive staining in the conjunctival epithelium. However, 50-week-old *Sod1*$^{-/-}$ mice showed scanty positive staining in the conjunctival epithelium (Fig. 3C). Real-time RT-PCR of the conjunctival tissues showed that Muc5ac mRNA expression in the 10-week-old *Sod1*$^{-/-}$ mice was significantly higher than the 10-week-old WT mice ($P = 0.0192$). On the other hand, Muc5ac mRNA expression in the 50-week-old *Sod1*$^{-/-}$ mice was lower than the 50-week-old WT mice ($P = 0.0076$). In the 50-week-old *Sod1*$^{-/-}$ mice, Muc5ac mRNA expression was significantly lower than 10-week-old *Sod1*$^{-/-}$ mice ($P < 0.0001$; Fig. 3D).

Electron Microscopy Revealed Marked Ultrastructural Alterations in Aged *Sod1*$^{-/-}$ Mice Conjunctiva

Conjunctival specimens from the 50-week-old WT and *Sod1*$^{-/-}$ mice were observed under transmission electron microscopy. The specimens from the WT mice showed a normal architecture of the conjunctival epithelium with abundant goblet cells (Figs. 4A, 4C). In the *Sod1*$^{-/-}$ mice conjunctival epithelium, marked thickening of the conjunctival epithelium and goblet cell loss were observed (Fig. 4B). Figure 4C shows normal microvilli and goblet cell secretory mucin packages. Flattening of the superficial conjunctival epithelium, blunting of microvilli, and decreased intercellular cohesion between the conjunctival epithelial cells were prominent in the 50-week-old *Sod1*$^{-/-}$ mice (Fig. 4D). Figure 4E shows normal basement membrane architecture in the 50-week-old WT mice. Distortion and thickening of the basement membrane in the 50-week-old *Sod1*$^{-/-}$ mice was also observed beneath the conjunctival basal epithelium (Fig. 4F).

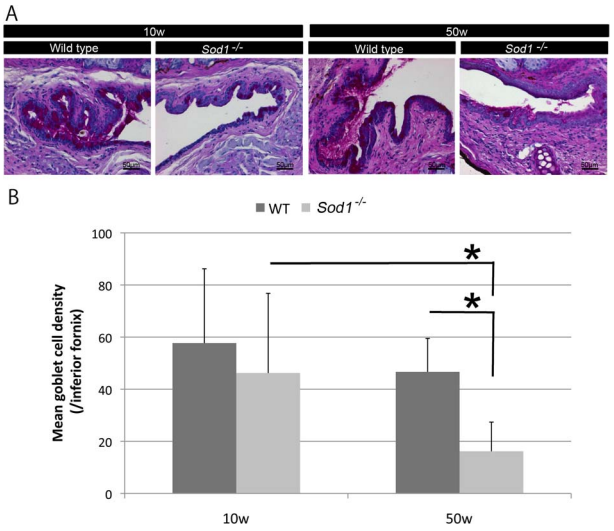

Figure 2. Goblet cells in the conjunctival epithelium of the *Sod1*$^{-/-}$ and WT mice. (**A**) Representative PAS-stained conjunctival specimens showed that PAS-positive goblet cells were scanty in the 50-week-old *Sod1*$^{-/-}$ mice. Please also note the thickening of conjunctival epithelium in the 50-week-old *Sod1*$^{-/-}$ mice. Hematoxylin staining was performed for counterstaining. (**B**) The mean number of goblet cells in the 50-week-old *Sod1*$^{-/-}$ mice was less than either the 10-week-old *Sod1*$^{-/-}$ mice or the 50-week-old WT mice. *$P < 0.05$.

Aging Was Associated With Alterations of mRNA Expression in Keratinization or Goblet Cell Differentiation Markers in *Sod1*$^{-/-}$ Mice

To quantify the mRNA expression related to goblet cell differentiation and keratinization, real-time RT-PCR was performed. The mRNA expression of Spdef, a transcription factor related to goblet cell differentiation, in the 10-week-old *Sod1*$^{-/-}$ mice was significantly higher than the 10-week-old WT mice ($P < 0.0001$). The Spdef expression in the 50-week-old *Sod1*$^{-/-}$ mice was significantly lower than the 50-week-old WT mice ($P = 0.0016$). The Spdef expression in the 50-week-old *Sod1*$^{-/-}$ mice was significantly lower than the 10-week-old *Sod1*$^{-/-}$ mice ($P < 0.0001$; Fig. 5A). The mRNA expression of involcurin, a keratinization-related protein, in the 50-week-old *Sod1*$^{-/-}$ mice was significantly higher than the 10-week-old *Sod1*$^{-/-}$ mice ($P < 0.0001$). The involucrin expression in the *Sod1*$^{-/-}$ mice showed a significant reduction from 10 to 50 weeks ($P < 0.0001$). The mRNA expression of transglutaminase 1, a keratinization-related protein, in the 50-week-old *Sod1*$^{-/-}$ mice was significantly higher than the 50-week-old WT mice ($P < 0.0001$). The transglutaminase 1 expression showed a significant increase from 10 to 50 weeks in the *Sod1*$^{-/-}$ mice ($P < 0.0001$).

Discussion

Oxidative stress is defined as the imbalance between production of reactive oxygen species and restoration by antioxidant systems. Previous experimental animal studies proposed that Cu, Zn-*SOD* knockout (*Sod1*$^{-/-}$) caused an elevated oxidative stress status, resulting in various aging phenotypes such as muscle atrophy,[12] macular degeneration,[13] fat liver deposits,[14] hepatic carcinoma[15] and hemolytic anemia,[16] skin atrophy,[17] bone loss,[18,19] exacerbation of Alzheimer's disease,[20] and rotator cuff degeneration.[21] In humans, oxidative stress has been reported to be involved in many systemic diseases including Parkinson's disease,[22] Alzheimer's disease,[23] amyotrophic lateral sclerosis,[24] cardiovascular diseases,[25] cancer,[26,27] and ischemic disorders.[28,29] Oxygen free radical and antioxidant systems have also been demonstrated to be potentially important in the pathogenesis of ocular diseases such as cataract,[30] age-related macular degeneration,[13] glaucoma,[31] and dry eye disease.[10] We previously demonstrated that excessive accumulation of oxidative stress led to histopathologic alterations in the lacrimal glands and deteriorated lacrimal gland functions in the *Sod1*$^{-/-}$ mice.[10]

Healthy conjunctival tissues can contribute to tear film stability. The membrane mucins can alter the innermost surface of conjunctival epithelium to a hydrophilic status, and secreted mucins spread into the aqueous layer and stabilize the tear film. Both membrane and secreted mucins also contribute to the barrier functions against foreign pathogens.

A recent study using in vivo confocal microscopy revealed that there was a negative correlation between goblet cell

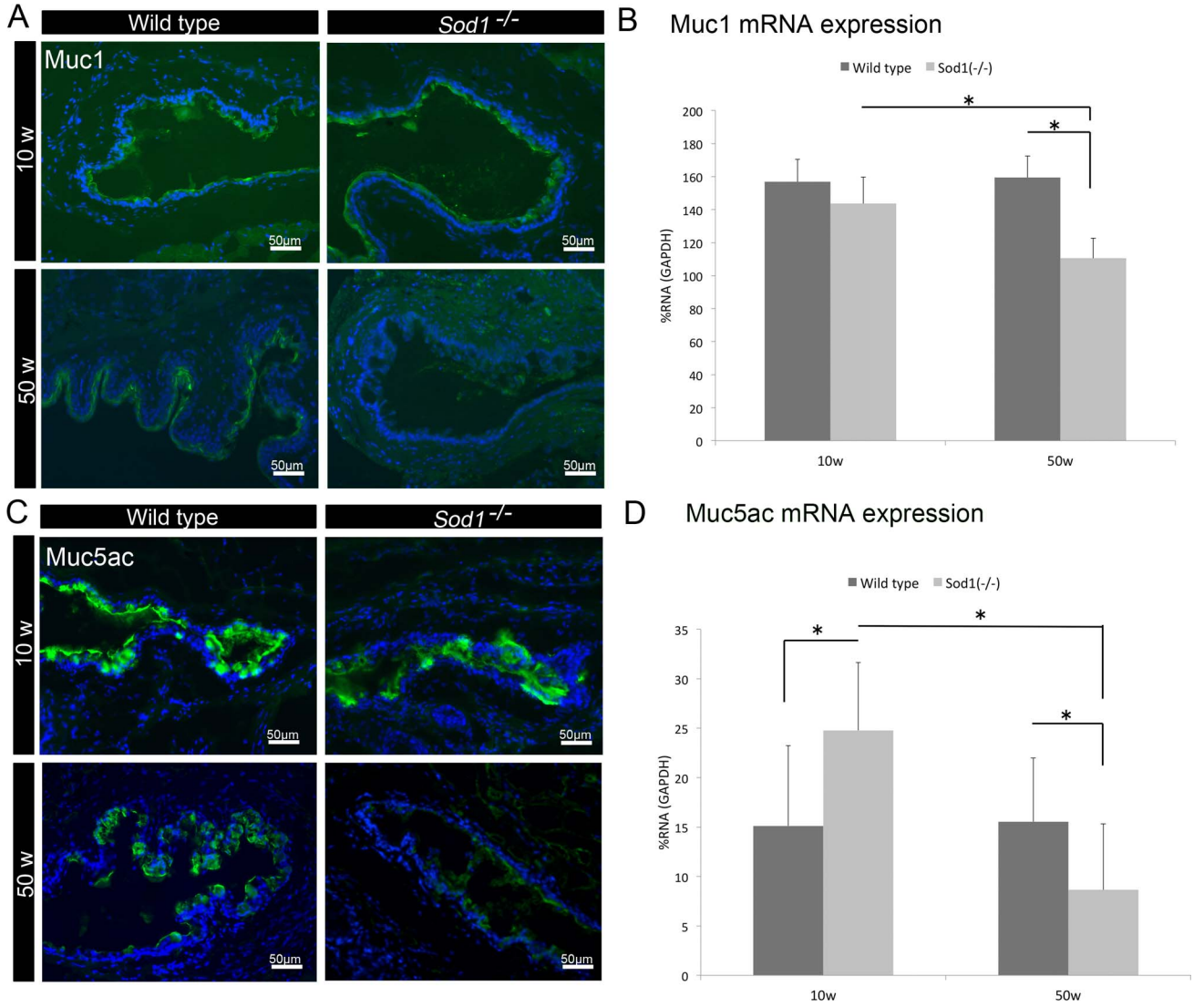

Figure 3. Immunohistochemistry staining and conjunctival mucin expression changes with aging in the *Sod1*$^{-/-}$ and WT mice. (**A**) The surface of the conjunctival epithelium was densely stained with membrane tethered mucin Muc1 in the 10-week-old *Sod1*$^{-/-}$ and WT mice. Note the relatively scanty staining in the representative specimen from the *Sod1*$^{-/-}$ mice at 50 weeks compared with the WT mice. DAPI was used for nuclear staining. (**B**) The mean Muc1 mRNA expression in the 10-week-old *Sod1*$^{-/-}$ mice showed no difference compared with 10-week-old WT mice. Note the Muc1 mRNA expression in the 50-week-old *Sod1*$^{-/-}$ mice was significantly less than the WT mice. (**C**) Abundant secreted mucin Muc5ac was densely stained in the 10-week-old *Sod1*$^{-/-}$ and WT mice. Note the relatively scanty staining cells in the specimen from the *Sod1*$^{-/-}$ mice at 50 weeks compared with the WT mice. DAPI was used for nuclear staining. (**D**) The mean Muc5ac mRNA expression in the 10-week-old *Sod1*$^{-/-}$ mice was significantly higher than the 10-week-old WT mice. On the other hand, Muc5ac mRNA expression in 50-week-old *Sod1*$^{-/-}$ mice was significantly less than the 50-week-old WT mice. *$P < 0.05$.

density in the conjunctiva and aging.[32] Previous literature showed that goblet cell densities decreased with various type of dry eyes including Sjögren syndrome, Stevens Johnson syndrome, and graft-versus-host disease.[33–35]

Several reports showed that the incidence of dry eye disease increases with age. The prevalence of dry eye disease (DES) in US women younger than 50 years old was 5.7% and was 9.8% among women older than 75 years old.[36] In the DEWS report, aging is defined as one of the environmental factors to cause dry eye disease.

In the current study, we confirmed a decrease in tear volume and an increase in fluorescein staining score in the 50-week-old *Sod1*$^{-/-}$ mice. These data were consistent with previous reports from our laboratory.[10] In addition to the tear volume and ocular surface abnormality, the current study revealed that tear film BUT was deteriorated in the 50-week-old *Sod1*$^{-/-}$ mice. Generally, an unstable tear film is considered to be caused by aqueous tear deficiency, excessive tear evaporation, or alteration of ocular surface mucins. In the current study, we found a significant decrease in the number of goblet cells in aged *Sod1*$^{-/-}$ mice. Moreover, a decreased intensity of immunohistochemistry stainings with Muc1 and Muc5ac in the aged *Sod1*$^{-/-}$ mice concomitant with a decrease in mRNA expression levels of Muc1 and Muc5ac was observed. These changes coexisted with accumulation of oxidative stress in the conjunctiva, which might have affected conjunctival mucins and deteriorated the tear film stability.

The conjunctival PAS staining in the *Sod1*$^{-/-}$ mice showed thickening of the conjunctival epithelium and a decrease of goblet cell density with aging. Transmission electron micros-

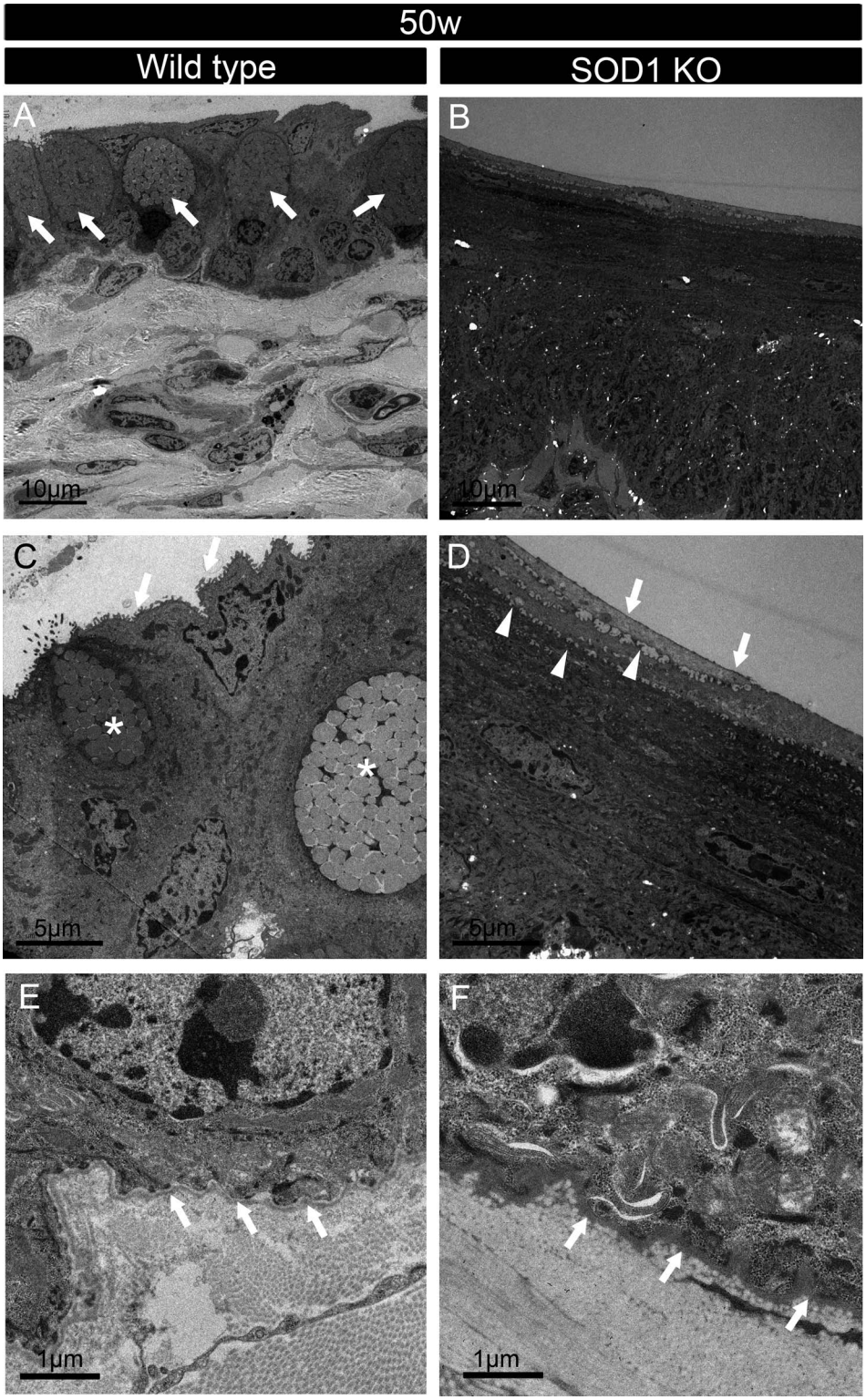

Figure 4. Transmission electron microscopy evaluations of the conjunctival tissues in the 50-week-old WT and *Sod1*$^{-/-}$ mice. The WT mice showed normal architecture of the conjunctival epithelium with abundant goblet cells ([**A**], *arrows*; [**C**], *asterisks*), microvilli ([**C**], *arrows*), and a smooth and thin layer of the basement membrane ([**E**], *arrows*). On the other hand, marked thickening of conjunctival epithelium and goblet cell loss were observed in the *Sod1*$^{-/-}$ mice (**B**). Flattening of the superficial conjunctival epithelium, blunting of microvilli ([**D**], *arrows*), and decreased cohesion of the conjunctival epithelium ([**D**], *arrowheads*) were prominent in the *Sod1*$^{-/-}$ mice (**D**). Distortion and thickening of the basement membrane in *Sod1*$^{-/-}$ mice was also observed beneath the conjunctival basal epithelium ([**F**], *arrows*).

Investigative Ophthalmology & Visual Science

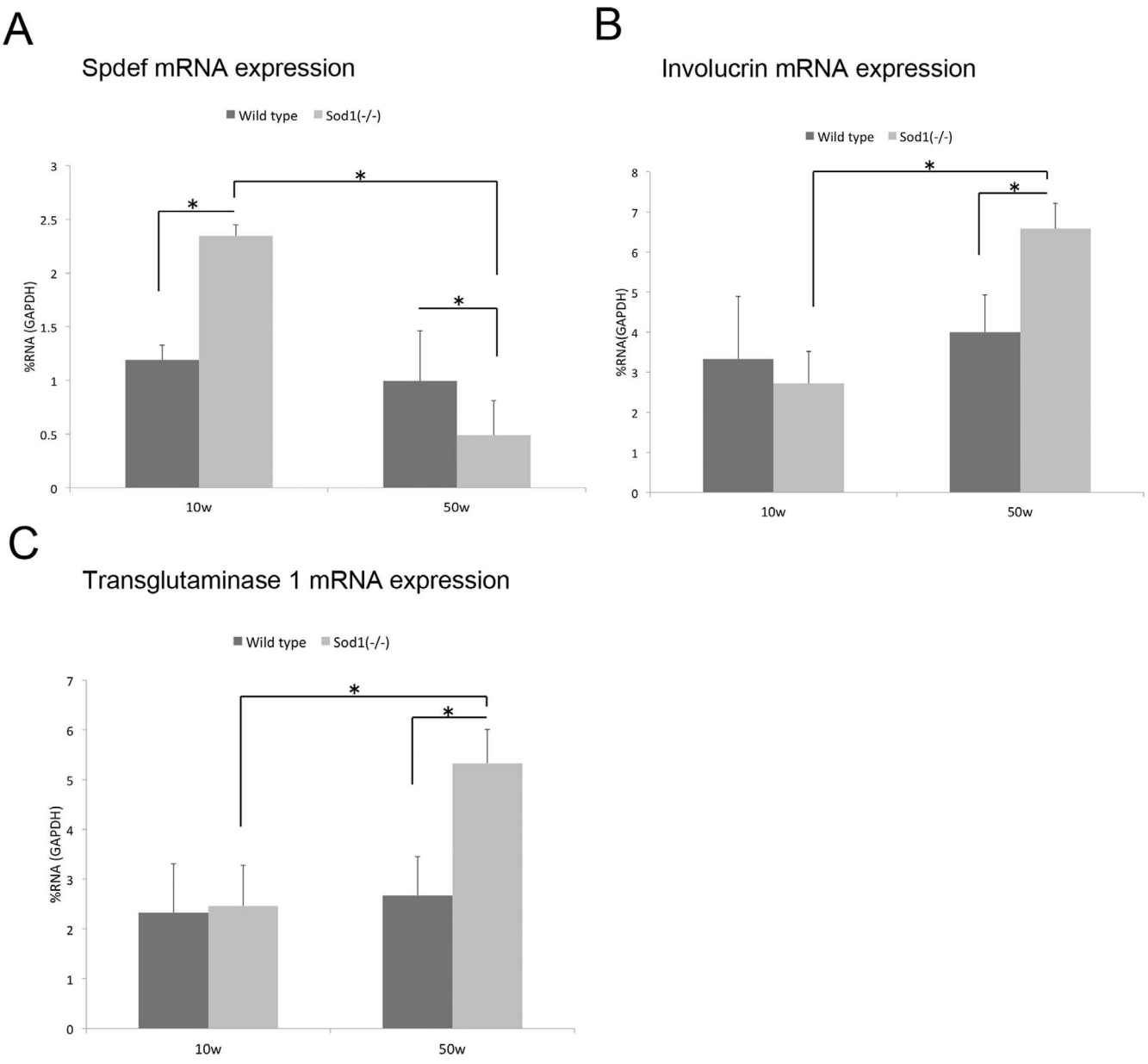

Figure 5. Real-time RT-PCR evaluations of goblet cell differentiation and keratinization in the conjunctival tissues. Spdef expression in the 50-week-old *Sod1*$^{-/-}$ mice was significantly less than the 50-week-old WT mice or the 10-week-old *Sod1*$^{-/-}$ mice. Fifty-week-old WT mice showed a higher Spdef mRNA expression than the 10-week-old WT mice (**A**). Involucrin mRNA expression in the 50-week-old *Sod1*$^{-/-}$ mice was higher than the 50-week-old WT mice or the 10-week-old *Sod1*$^{-/-}$ mice (**B**). The mRNA expression of transglutaminase 1 in the 50-week-old *Sod1*$^{-/-}$ mice was significantly higher than the 50-week-old WT mice or the 10-week-old WT mice (**C**). *$P < 0.05$.

copy also confirmed the decrease of goblet cells and thickening of the conjunctival epithelium. Transmission electron microscopy observations further revealed weakening of intercellular cohesion in the uppermost layer of conjunctival epithelium. The basement membrane of the conjunctival epithelium in the 50-week-old *Sod1*$^{-/-}$ mice was distorted and became thicker compared with the same aged WT mice.

In the current study, we found notable findings in relation to the mRNA expression in the young and older aged *Sod1*$^{-/-}$ mice. Muc5ac and Spdef mRNA expression in the 10-week-old *Sod1*$^{-/-}$ mice was significantly higher than the 10-week-old WT mice. On the other hand, Muc5ac and Spdef mRNA expression in the 50-week-old *Sod1*$^{-/-}$ mice was significantly lower than the 50-week-old WT mice. These findings suggest a decline in epithelial differentiation with aging in the *Sod1*$^{-/-}$ mice. It might be that, with aging, the conjunctival epithelium may gradually undergo an alteration of phenotype due to accumulation of oxidative stress.

To further investigate the mechanism of goblet cell loss in aged *Sod1*$^{-/-}$ mice, Spdef mRNA expression was measured. Aged *Sod1*$^{-/-}$ mice showed a decrease of Spdef mRNA expression in the conjunctival tissue compared with aged WT mice. Accumulation of oxidative stress in the conjunctival epithelium could alter the Spdef expression and induce phenotypic alterations toward a squamous metaplastic epithelium. Indeed, increased mRNA expression of keratinization-related proteins (transglutaminase 1 and involucrin) in the aged *Sod1*$^{-/-}$ mice could be caused by desiccation stress due to

the low wettability of the ocular surface. In epidermal tissue, a cornified cell envelope was formed underneath the plasma membrane and consisted of cornified precursor proteins such as involcurin and loricrin. These precursor proteins are cross-linked by transglutaminase 1. Although the existence of a cornified cell envelope was still unknown in the ocular surface, in severe ocular surface diseases, such as Stevens Johnson syndrome and ocular cicatricial pemphigoid, elevation of transglutaminase 1 mRNA expression and increased cornified precursor protein involcurin were reported.[37] A detailed pathogenesis of keratinization-related mRNA and protein up-regulation in severe ocular surface disease is still unknown. Because dry eye disease is one of the major diseases causing squamous metaplasia, dryness of the ocular surface may be involved in the pathogenesis of the keratinization process in severe ocular surface disease. Another study showed that mice with an experimental dry eye model showed increased mRNA expression of cornified envelope precursor proteins, cross-linking transglutaminase 1 enzyme, and decreased mRNA expression of Muc5ac.[38] Aged *Sod1*$^{-/-}$ mice showed the phenotype of dry eye disease including decreased tear volume, decreased tear stability, and ocular surface damage. It is possible that dry eye in the aged *Sod1*$^{-/-}$ mice caused a phenotypic alteration in the conjunctival tissues into squamous metaplasia.

A few potential limitations were apparent in our study. Only male mice were analyzed to avoid the effect of menstrual cycle in the study. Because dry eye is more prevalent in women, we need to investigate female mice in the future studies.

In conclusion, accumulation of oxidative stress in the aged *Sod1*$^{-/-}$ mice induced a decrease of corneal wettability and altered the conjunctival epithelium to a squamous metaplastic phenotype. Further mechanisms of how oxidative stress affects Spdef expression with aging should be investigated in future studies.

Acknowledgments

The authors thank Y. Ozawa (Department of Advanced Aging Medicine, Chiba University Graduate School of Medicine) for logistic support in maintaining the knockout mice. The authors alone are responsible for the content and writing of the paper.

Disclosure: **T. Kojima**, None; **M. Dogru**, None; **O.M.A. Ibrahim**, None; **T.H. Wakamatsu**, None; **M. Ito**, None; **A. Igarashi**, None; **T. Inaba**, None; **T. Shimizu**, None; **T. Shirasawa**, None; **J. Shimazaki**, None; **K. Tsubota**, None

References

1. The epidemiology of dry eye disease: Report of the Epidemiology Subcommittee of the International Dry Eye WorkShop (2007). *Ocul Surf*. 2007;5:93–107.
2. Goto E, Yagi Y, Matsumoto Y, Tsubota K. Impaired functional visual acuity of dry eye patients. *Am J Ophthalmol*. 2002;133:181–186.
3. Paulsen AJ, Cruickshanks KJ, Fischer ME, et al. Dry eye in the beaver dam offspring study: prevalence, risk factors, and health-related quality of life. *Am J Ophthalmol*. 2014;157:799–806.
4. Li M, Gong L, Chapin WJ, Zhu M. Assessment of vision-related quality of life in dry eye patients. *Invest Ophthalmol Vis Sci*. 2012;53:5722–5727.
5. The definition and classification of dry eye disease: Report of the Definition and Classification Subcommittee of the International Dry Eye WorkShop (2007). *Ocul Surf*. 2007;5:75–92.
6. Koh S, Maeda N, Hirohara Y, et al. Serial measurements of higher-order aberrations after blinking in patients with dry eye. *Invest Ophthalmol Vis Sci*. 2008;49:133–138.
7. Droge W. Free radicals in the physiological control of cell function. *Physiol Rev*. 2002;82:47–95.
8. Crapo JD, Oury T, Rabouille C, Slot JW, Chang LY. Copper, zinc superoxide dismutase is primarily a cytosolic protein in human cells. *Proc Natl Acad Sci U S A*. 1992;89:10405–10409.
9. Fridovich I. Superoxide anion radical (O2-.), superoxide dismutases, and related matters. *J Biol Chem*. 1997;272:18515–18517.
10. Kojima T, Wakamatsu TH, Dogru M, et al. Age-related dysfunction of the lacrimal gland and oxidative stress: evidence from the Cu, Zn-superoxide dismutase-1 (Sod1) knockout mice. *Am J Pathol*. 2012;180:1879–1896.
11. Marko CK, Menon BB, Chen G, Whitsett JA, Clevers H, Gipson IK. Spdef null mice lack conjunctival goblet cells and provide a model of dry eye. *Am J Pathol*. 2013;183:35–48.
12. Muller FL, Song W, Liu Y, et al. Absence of CuZn superoxide dismutase leads to elevated oxidative stress and acceleration of age-dependent skeletal muscle atrophy. *Free Radic Biol Med*. 2006;40:1993–2004.
13. Imamura Y, Noda S, Hashizume K, et al. Drusen, choroidal neovascularization, and retinal pigment epithelium dysfunction in SOD1-deficient mice: a model of age-related macular degeneration. *Proc Natl Acad Sci U S A*. 2006;103:11282–11287.
14. Uchiyama S, Shimizu T, Shirasawa T. CuZn-SOD deficiency causes ApoB degradation and induces hepatic lipid accumulation by impaired lipoprotein secretion in mice. *J Biol Chem*. 2006;281:31713–31719.
15. Elchuri S, Oberley TD, Qi W, et al. CuZnSOD deficiency leads to persistent and widespread oxidative damage and hepatocarcinogenesis later in life. *Oncogene*. 2005;24:367–380.
16. Iuchi Y, Okada F, Onuma K, et al. Elevated oxidative stress in erythrocytes due to a SOD1 deficiency causes anaemia and triggers autoantibody production. *Biochem J*. 2007;402:219–227.
17. Murakami K, Inagaki J, Saito M, et al. Skin atrophy in cytoplasmic SOD-deficient mice and its complete recovery using a vitamin C derivative. *Biochem Biophys Res Commun*. 2009;382:457–461.
18. Nojiri H, Saita Y, Morikawa D, et al. Cytoplasmic superoxide causes bone fragility due to low turnover osteoporosis and impaired collagen cross-linking. *J Bone Miner Res*. 2011;26:2682–2694.
19. Morikawa D, Nojiri H, Saita Y, et al. Cytoplasmic reactive oxygen species and SOD1 regulate bone mass during mechanical unloading. *J Bone Miner Res*. 2013;28:2368–2380.
20. Murakami K, Murata N, Noda Y, et al. SOD1 (copper/zinc superoxide dismutase) deficiency drives amyloid beta protein oligomerization and memory loss in mouse model of Alzheimer disease. *J Biol Chem*. 2011;286:44557–44568.
21. Morikawa D, Itoigawa Y, Nojiri H, et al. Contribution of oxidative stress to the degeneration of rotator cuff entheses. *J Shoulder Elbow Surg*. 2014;23:628–635.
22. Schapira AH, Tolosa E. Molecular and clinical prodrome of Parkinson disease: implications for treatment. *Nat Rev Neurol*. 2010;6:309–317.
23. Higgins GC, Beart PM, Shin YS, Chen MJ, Cheung NS, Nagley P. Oxidative stress: emerging mitochondrial and cellular themes and variations in neuronal injury. *J Alzheimers Dis*. 2010;20(suppl 2):S453–S473.
24. Deng HX, Shi Y, Furukawa Y, et al. Conversion to the amyotrophic lateral sclerosis phenotype is associated with intermolecular linked insoluble aggregates of SOD1 in mitochondria. *Proc Natl Acad Sci U S A*. 2006;103:7142–7147.
25. Milei J, Forcada P, Fraga CG, et al. Relationship between oxidative stress, lipid peroxidation, and ultrastructural damage in patients with coronary artery disease undergoing cardioplegic arrest/reperfusion. *Cardiovasc Res*. 2007;73:710–719.

26. Reuter S, Gupta SC, Chaturvedi MM, Aggarwal BB. Oxidative stress, inflammation, and cancer: how are they linked? *Free Radic Biol Med*. 2010;49:1603–1616.
27. Pavlides S, Tsirigos A, Migneco G, et al. The autophagic tumor stroma model of cancer: role of oxidative stress and ketone production in fueling tumor cell metabolism. *Cell Cycle*. 2010; 9:3485–3505.
28. Chong ZZ, Shang YC, Hou J, Maiese K. Wnt1 neuroprotection translates into improved neurological function during oxidant stress and cerebral ischemia through AKT1 and mitochondrial apoptotic pathways. *Oxid Med Cell Longev*. 2010;3:153–165.
29. Ying W, Xiong ZG. Oxidative stress and NAD+ in ischemic brain injury: current advances and future perspectives. *Curr Med Chem*. 2010;17:2152–2158.
30. Spector A. Oxidative stress-induced cataract: mechanism of action. *Faseb J*. 1995;9:1173–1182.
31. Yuki K, Ozawa Y, Yoshida T, et al. Retinal ganglion cell loss in superoxide dismutase 1 deficiency. *Invest Ophthalmol Vis Sci*. 2011;52:4143–4150.
32. Wei A, Hong J, Sun X, Xu J. Evaluation of age-related changes in human palpebral conjunctiva and meibomian glands by in vivo confocal microscopy. *Cornea*. 2011;30:1007–1012.
33. Gipson IK, Hori Y, Argueso P. Character of ocular surface mucins and their alteration in dry eye disease. *Ocul Surf*. 2004; 2:131–148.
34. Nelson JD, Wright JC. Conjunctival goblet cell densities in ocular surface disease. *Arch Ophthalmol*. 1984;102:1049–1051.
35. Wang Y, Ogawa Y, Dogru M, et al. Baseline profiles of ocular surface and tear dynamics after allogeneic hematopoietic stem cell transplantation in patients with or without chronic GVHD-related dry eye. *Bone Marrow Transplant*. 2010;45:1077–1083.
36. Schaumberg DA, Sullivan DA, Buring JE, Dana MR. Prevalence of dry eye syndrome among US women. *Am J Ophthalmol*. 2003;136:318–326.
37. Nakamura T, Nishida K, Dota A, Matsuki M, Yamanishi K, Kinoshita S. Elevated expression of transglutaminase 1 and keratinization-related proteins in conjunctiva in severe ocular surface disease. *Invest Ophthalmol Vis Sci*. 2001;42:549–556.
38. Corrales RM, de Paiva CS, Li DQ, et al. Entrapment of conjunctival goblet cells by desiccation-induced cornification. *Invest Ophthalmol Vis Sci*. 2011;52:3492–3499.

Investigative Ophthalmology & Visual Science